



PAPER • OPEN ACCESS

## Muon spin rotation and relaxation study on topological noncentrosymmetric superconductor $\text{PbTaSe}_2$

To cite this article: Z H Zhu *et al* 2022 *New J. Phys.* **24** 023002

View the [article online](#) for updates and enhancements.

You may also like

- [Electron-phonon superconductivity in C-doped topological nodal-line semimetal  \$\text{Zr}\_2\text{Pt}\_3\$ : a muon spin rotation and relaxation \(SR\) study](#)  
A Bhattacharyya, P P Ferreira, K Panda et al.
- [SR Study of Organic Superconductor -  \$\(\text{BETS}\)\_x\text{GaCl}\_4\$](#)   
D P Sañi, R Asih, S S Mohm-Tajudin et al.
- [Muonium as a model for interstitial hydrogen in the semiconducting and semimetallic elements](#)  
S F J Cox



## PAPER

Muon spin rotation and relaxation study on topological noncentrosymmetric superconductor PbTaSe<sub>2</sub>

## OPEN ACCESS

## RECEIVED

12 October 2021

## REVISED

23 December 2021

## ACCEPTED FOR PUBLICATION

6 January 2022


## PUBLISHED

31 January 2022

Original content from this work may be used under the terms of the [Creative Commons Attribution 4.0 licence](#).

Any further distribution of this work must maintain attribution to the author(s) and the title of the work, journal citation and DOI.



Z H Zhu<sup>1</sup>, C Tan<sup>1</sup>, J Zhang<sup>1</sup>, P K Biswas<sup>2,3</sup> , A D Hillier<sup>3</sup>, M X Wang<sup>1</sup>, Y X Yang<sup>1</sup>, C S Chen<sup>1</sup>, Z F Ding<sup>1</sup>, S Y Li<sup>1,4,5</sup> and L Shu<sup>1,4,5,\*</sup> 

<sup>1</sup> State Key Laboratory of Surface Physics, Department of Physics, Fudan University, Shanghai 200433, People's Republic of China

<sup>2</sup> Laboratory for Muon Spin Spectroscopy, Paul Scherrer Institute, CH-5232 Villigen PSI, Switzerland

<sup>3</sup> ISIS Pulsed Neutron and Muon Source, STFC Rutherford Appleton Laboratory, Harwell Campus, Didcot, Oxfordshire OX11 0QX, United Kingdom

<sup>4</sup> Collaborative Innovation Center of Advanced Microstructures, Nanjing 210093, People's Republic of China

<sup>5</sup> Shanghai Research Center for Quantum Sciences, Shanghai 201315, People's Republic of China

\* Author to whom any correspondence should be addressed.

E-mail: [leishu@fudan.edu.cn](mailto:leishu@fudan.edu.cn)

**Keywords:** topological, noncentrosymmetric superconductivity, muon spin relaxation/rotation

## Abstract

Topological superconductivity is an exotic phenomenon due to the symmetry-protected topological surface state, in which a quantum system has an energy gap in the bulk but supports gapless excitations confined to its boundary. Symmetries including central and time-reversal symmetry (TRS), along with their relations with topology, are crucial for topological superconductivity. We report muon spin relaxation/rotation ( $\mu$ SR) experiments on a topological noncentrosymmetric superconductor PbTaSe<sub>2</sub> to study its TRS and gap symmetry. Zero-field  $\mu$ SR experiments indicate the absence of internal magnetic field in the superconducting state, consistent with previous  $\mu$ SR results. Furthermore, transverse-field  $\mu$ SR measurements reveals that the superconducting gap of PbTaSe<sub>2</sub> is an isotropic three-dimensional fully-gapped single-band. The fully-gapped results can help understand the pairing mechanism and further classify the topological superconductivity in this system.

## 1. Introduction

In unconventional superconductors, symmetries in addition to U(1) gauge symmetry are broken in the superconducting state, leading to exotic and potentially useful properties, therefore realization and study of superconductivity in systems with reduced symmetry is one of the most crucial research field. Among these, noncentrosymmetric crystal structures with significant spin-orbital coupling are of particular interest [1]. In superconductors with noncentrosymmetric crystal structures, the absence of inversion symmetry leads to the splitting of the Fermi surfaces into two opposite spin configurations, and results in the mixed singlet–triplet nature in the order parameter [1–4]. As a result, it can give rise to a range of novel phenomena, including the recently proposed topological superconductivity [5–8].

Topological superconductivity is an exotic phenomenon due to the symmetry-protected topological surface state [9]. In a topological superconductor, the bulk state is a fully gapped superconducting state, while the surface state is a metal state. The Hamiltonian of such state is defined by several important symmetries. The most important symmetry for a topological material is time-reversal symmetry (TRS), which determines the topological mode of the material [9]. TRS is also one of the most intensely studied symmetries for a superconductor, and has been observed in a handful of weakly correlated noncentrosymmetric superconductors [10–15]. Despite broken TRS being a clear signature of unconventional superconductivity was observed, many other properties resemble conventional superconductors. This immediately raises an important question, namely what is the origin of the TRS breaking in this kind of material, or does TRS breaking occur together with a conventional electron–phonon pairing mechanism? Furthermore, the relationship between TRS breaking and breaking

inversion symmetry requires clarification since there are also examples in which TRS breaking occurs in centrosymmetric systems [16].

Recently, a noncentrosymmetric superconductor PbTaSe<sub>2</sub> with transition temperature  $T_c = 3.7$  K was reported to host a  $\mathbb{Z}_2$  topological state with topological nodal-line state by *ab initio* calculations, angle-resolved photoemission spectroscopy (ARPES) and soft point-contact spectroscopy experiments [17–22]. Zero-field (ZF) muon spin relaxation ( $\mu$ SR) measurement shows no evidence for a TRS breaking field greater than 0.05 G in the superconducting state [23]. Different techniques, including specific heat and nuclear magnetic resonance (NMR) measurements [17, 24], agree with an in-plane fully gapped superconducting state of PbTaSe<sub>2</sub>. A recent calculation work suggests multi-band superconductivity due to the complex band structure revealed by ARPES [18, 19, 25]. However, experimentally it remains controversial whether it is single band or multi-band superconductor. The tunnel diode oscillator experiment supports single band [26], but the thermal conductivity measurement suggests multi-band picture [27]. In addition, while both scanning tunnel microscopy (STM) and  $\mu$ SR results can be described by either single or multi-band model, STM result gives similar magnitude of gap values from different bands, and  $\mu$ SR result indicates two different gaps [20, 23].

It is worth noting that PbTaSe<sub>2</sub> is a three-dimensional material with strong anisotropic behavior [28]. All the superconducting pairing symmetry studies of PbTaSe<sub>2</sub> were in *ab*-plane so far, due to the limitation of measurement along the *c*-direction. It is particularly important to perform the gap symmetry study along *c*-direction, to clarify the relationship between topology, TRS, and superconducting pairing symmetry of this noncentrosymmetric superconductor.

We report the  $\mu$ SR experiment results on single crystalline PbTaSe<sub>2</sub>. No evidence of TRS breaking is confirmed. We find fully-gapped superconductivity in both in-plane and out-of-plane directions. Our results prefer the single-band picture. Most intriguingly, the normalized superfluid density in two directions have exactly same temperature dependence, suggesting a possible isotropic three-dimensional gap.

## 2. Experimental details

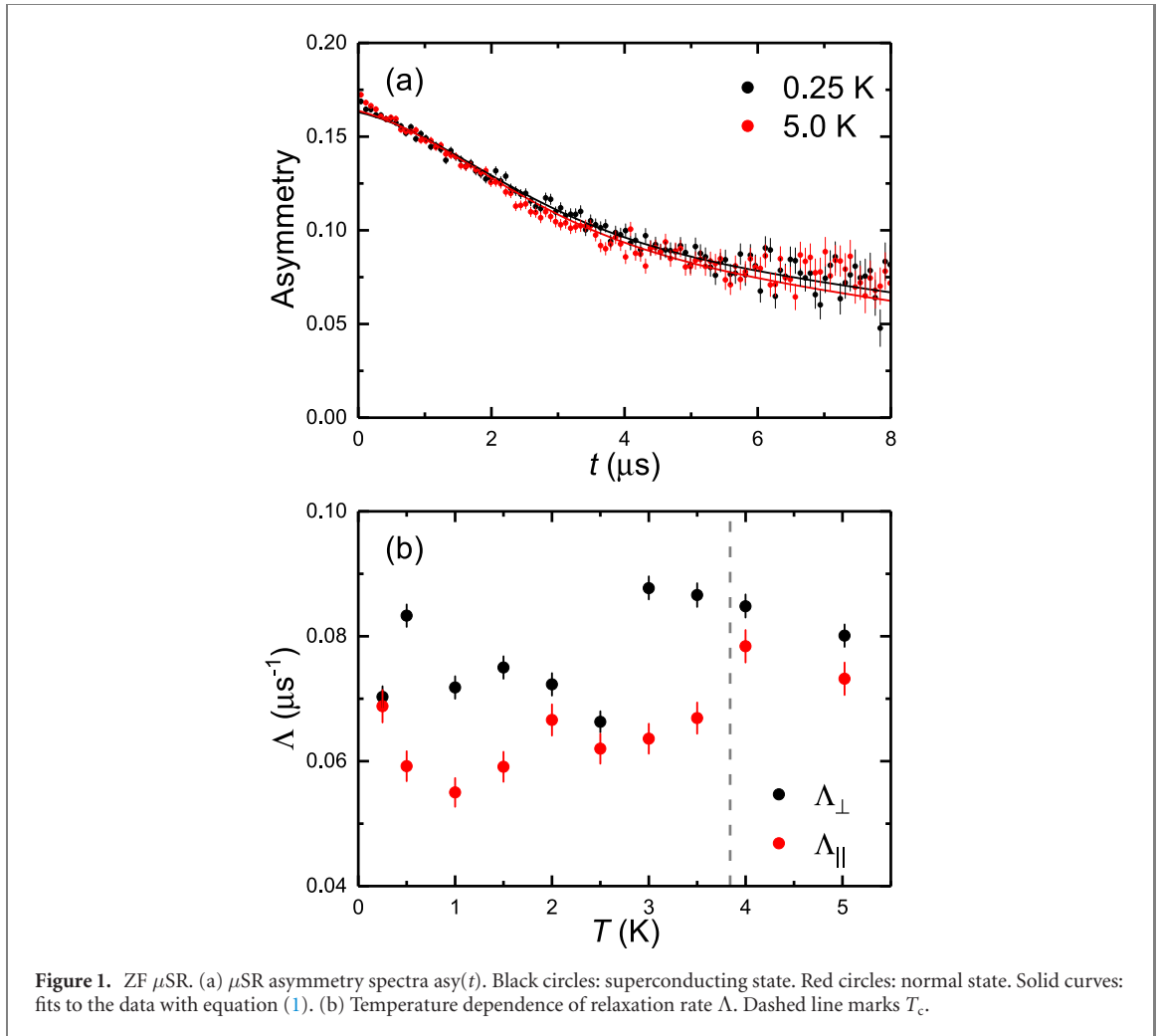
PbTaSe<sub>2</sub> single crystals were grown by the chemical vapor transport method as previously reported [18]. The typical size of obtained single crystals is  $5 \times 5 \times 0.02$  mm<sup>3</sup>. The quality of the single crystals was checked by x-ray diffraction, magnetic susceptibility and resistivity measurements [27].

$\mu$ SR experiments were performed at the DOLLY beam line at Paul Scherrer Institute, Villigen, Switzerland. A mosaic of single crystals were stacked and aligned with the (001) basal plane attached to a copper sample holder using dilute GE varnish. Helium-3 cryostat was used to cool the sample down to 0.25 K. In a  $\mu$ SR experiment, spin-polarized positive muons are implanted into a sample. On decay of the muon after an average lifetime of 2.2  $\mu$ s, a positron is emitted preferentially along the direction of the muon spin. The time evolution of muon spin polarization is determined by detecting decay positrons from an ensemble of  $1\text{--}2 \times 10^7$  muons. The functional form of the muon spin polarization depends on the spatial distribution and dynamical fluctuations of the muon magnetic environment.

During the experiments, the initial muon spin is 45° from the *c*-axis, which was surrounded by four detectors: forward, backward, up, and down. Hence we can measure the muon spin polarization along two different directions, i.e. parallel and perpendicular to the *c*-axis. As a trade, due to the angle between muon spin and detectors, the initial asymmetry in our experiments is much lower than the common value that is about 0.25. ZF  $\mu$ SR was performed above and below  $T_c$  to study whether there is spontaneous small magnetic field in the superconducting state due to the TRS breaking [10, 29, 30].

In transverse-field (TF)  $\mu$ SR experiments, an external magnetic field  $\mu_0 H$  (field cooled from above  $T_c$  in a superconductor) was applied to induce a flux-line lattice (FLL) where the internal magnetic field distribution is determined by the magnetic penetration depth  $\lambda$ , the vortex core radius and the structure of the FLL. The external field  $\mu_0 H$  should be between  $\mu_0 H_{c1}$  and  $\mu_0 H_{c2}$ . In our case,  $\mu_0 H_{c1}$  is about 4–9 mT [17, 23, 28],  $\mu_0 H_{c2}$  along *c*-axis is about 0.32 T, and  $\mu_0 H_{c2}$  parallel to *ab*-plane is about 1.25 T [28].

The  $\mu$ SR rate is related to the root-mean-square width of the internal magnetic field distribution in the FLL, and hence also related to  $\lambda$ , the details of which will be discussed after presenting the experimental results. We first applied magnetic field parallel to *c*-axis to obtain the penetration depth in the *ab*-plane and study the gap symmetry in that direction [31], and compare with the published work [23]. Then we apply an external field normal to *c*-axis. Since the samples were not aligned along *a* or *b*-axes, the gap symmetry in *ac* or *bc*-plane cannot be obtained. Instead, we obtained the average gap symmetry in planes that includes *c*-axis but with random directions in *ab*-plane. If there is any node in the superconducting gap out of *ab*-plane, the temperature dependence of superfluid density should deviate from the *s*-wave behavior.



The  $\mu$ SR data were analyzed with musfit software package [32].

### 3. Results

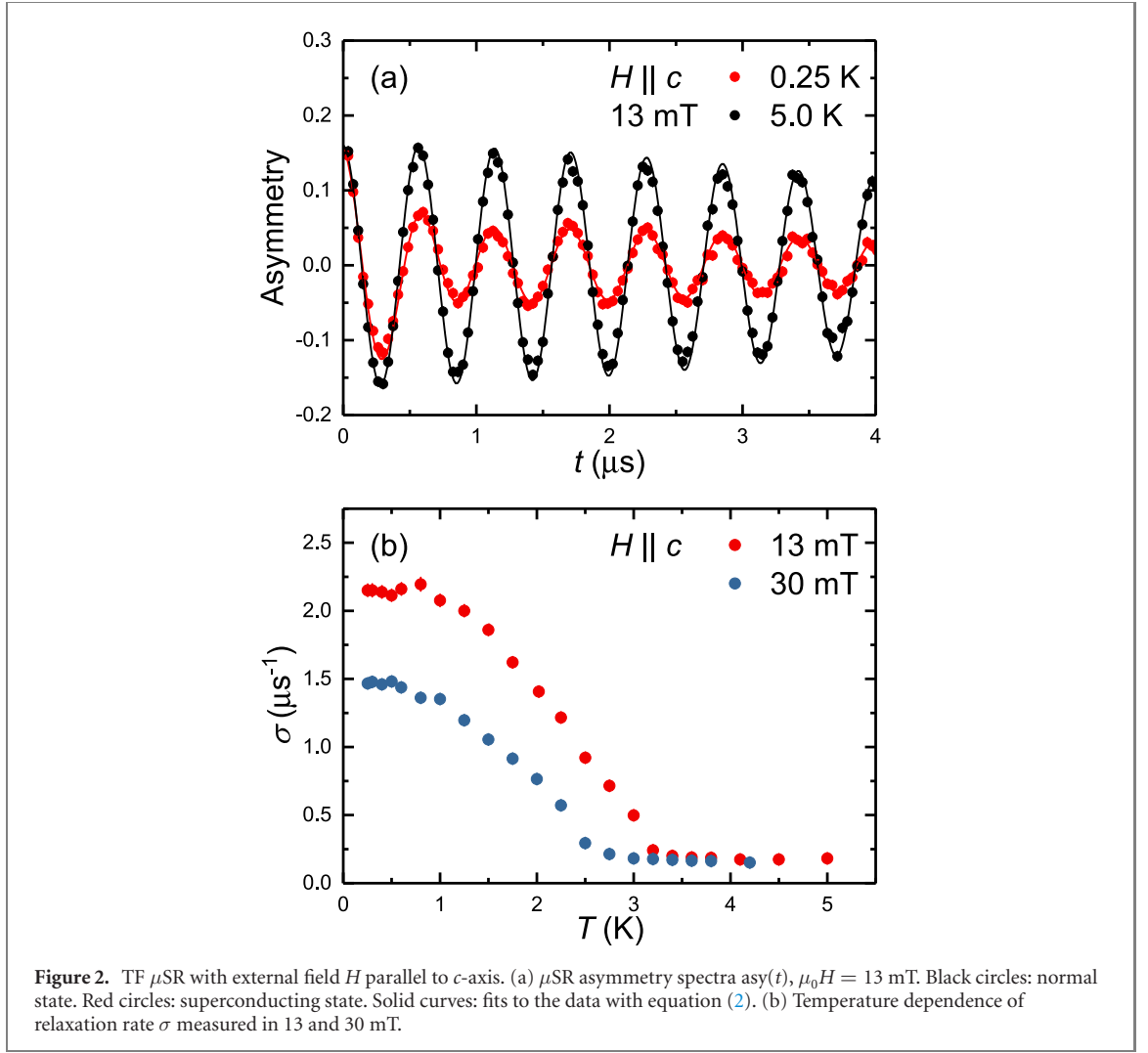
#### 3.1. ZF- $\mu$ SR

Representative ZF asymmetry time spectra at selective temperatures are shown in figure 1(a). No significant difference can be observed between the data above and below  $T_c = 3.84$  K. The  $\mu$ SR asymmetry spectrum consists of two contributions: a signal from muons stop in the sample and a slowly relaxing background signal from muons that stop in the copper sample holder. The spectra in both directions can be well described by the function

$$asy(t) = a_0[f \exp(-\Lambda t) + (1 - f)G_{KT}^{dyn}(\sigma_{Cu}^{ZF}, \nu, t)], \quad (1)$$

where the first and second terms represent sample and background signals, respectively. Here  $a_0$  is the initial asymmetry, and  $f$  denotes the fraction of muons stopping in the sample. The data of the first  $0.1 \mu s$  is dropped to avoid the early-time problems. The temperature independent  $f = 0.68$  is determined from TF- $\mu$ SR. The dynamic ZF Kubo–Toyabe (KT) function  $G_{KT}^{dyn}$ , which was used previously to fit ZF- $\mu$ SR data of Cu [33–35], describes the data adequately. We obtain  $\sigma_{Cu}^{ZF} = 0.38 \mu s^{-1}$  and  $\nu = 0.4$  MHz, same as previously reported [34, 35].

The temperature dependence of the ZF relaxation rate  $\Lambda$  is shown in figure 1(b). Consistent with previous report [23], no significant change crossing  $T_c$  is observed down to 0.25 K in our study. Such results suggest that there is no spontaneous magnetic field appearing in the superconducting state. Therefore, there is no TRS breaking, excluding the existence of triplet pairing [23]. Recently, it is reported that although the positive charge of muon could modify the local environment in ZF- $\mu$ SR experiments, TRS property shown by  $\mu$ SR is intrinsic since the effect induced by muon's charge is several eV below Fermi energy, which is much larger than the magnitude of superconducting gap (at the decade of meV) [36].



### 3.2. TF- $\mu$ SR

#### 3.2.1. $H \parallel c$ -axis

Figure 2(a) shows the TF- $\mu$ SR muon spin precession signals at applied field of 13 mT in the normal and superconducting states of PbTaSe<sub>2</sub>. As seen in figure 2(a), in the superconducting state the damping of signal is enhanced due to the field broadening generated by the vortex lattice.

The TF- $\mu$ SR asymmetry spectra in PbTaSe<sub>2</sub> can be well described by the function

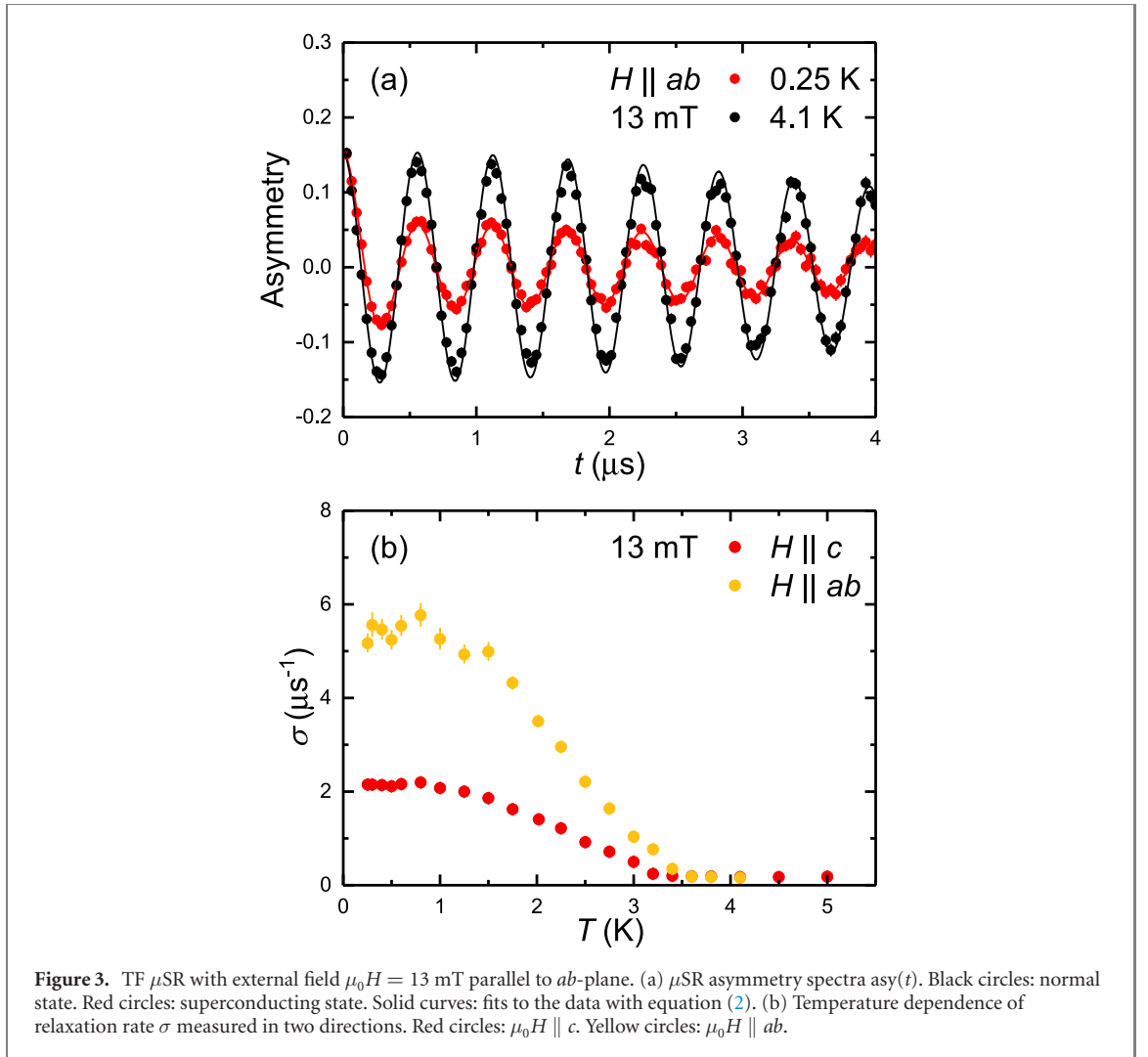
$$asy(t) = a_0 \left\{ f \exp \left[ -\frac{(\sigma t)^2}{2} \right] \cos(\gamma_\mu \mu_0 H_{\text{int}} t + \varphi) + (1 - f) \exp \left[ -\frac{(\sigma_{\text{Cu}}^{\text{TF}} t)^2}{2} \right] \cos(\gamma_\mu \mu_0 H t + \varphi) \right\}, \quad (2)$$

where the first and second terms represent sample and background signals, respectively. The relaxation rate of copper  $\sigma_{\text{Cu}}^{\text{TF}} = 0.24 \mu\text{s}^{-1}$  is also temperature independent, consistent with previous report [37]. The ratio of ZF and TF relaxation rate of copper is 1.58, consistent with the theoretical value [33]. The Gaussian relaxation rate  $\sigma$  from the sample is due to nuclear dipolar field in the normal state and it enhanced in the superconducting state by the vortex lattice.  $\gamma_\mu/2\pi = 135.5$  MHz/T is the gyromagnetic ratio of muon,  $H_{\text{int}}$  is the internal field, which is reduced due to diamagnetic screening. The curves in figure 2(a) are the fits of equation (2).

Temperature dependence of  $\sigma$  is shown in figure 2(b) at two different applied magnetic fields. The temperature independence of  $\sigma$  above  $T_c$  and the increase of  $\sigma$  with decreasing temperature below  $T_c$  are observed, indicating the bulk superconductivity occurs below  $T_c$ . The lower  $T_c$  in the 30 mT is consistent with the suppressing effect on superconductivity by external magnetic field.

#### 3.2.2. $H \parallel ab$ -plane

Similar results were obtained with field parallel to  $ab$ -plane, shown in figure 3. The  $\mu$ SR asymmetry spectra can also be well described by equation (2). However, compared with  $\sigma$  in 13 mT field along  $c$ -axis, the relaxation rate  $\sigma$  here is much larger, suggesting a much broader field distribution. Similar results were also



reported in  $\text{Mo}_3\text{P}$  [38]. Such difference between different directions can be attributed to the strong anisotropy of  $H_{c2}$  [31]. The estimated  $\mu_0 H_{c2}$  along  $c$ -axis is 0.32 T, while  $\mu_0 H_{c2}$  is 1.25 T parallel to  $ab$ -plane determined from electrical resistivity measurements [28]. In figure 3(b), the larger  $T_c$  measured at magnetic field parallel to  $ab$ -plane also indicate larger  $H_{c2}$  in that direction.

### 3.2.3. Pairing symmetry

The Gaussian relaxation rate  $\sigma$  is related to the Gaussian internal field distribution [33]. For a type-II superconductor in vortex state, the internal field distribution is convolution of contribution from the vortex lattice and nuclear dipole field distribution of the host material. Thus  $\sigma$  is given by

$$\sigma^2 = \sigma_{\text{SC}}^2 + \sigma_{\text{dip}}^2, \quad (3)$$

where  $\sigma_{\text{SC}}$  is the vortex lattice contribution, and  $\sigma_{\text{dip}}$  is temperature independent in the normal state and is not expected to change in the superconducting state. After determining  $\sigma_{\text{dip}} = 0.181(7) \mu\text{s}^{-1}$  from the normal state data, we can get temperature dependence of  $\sigma_{\text{SC}}$ .

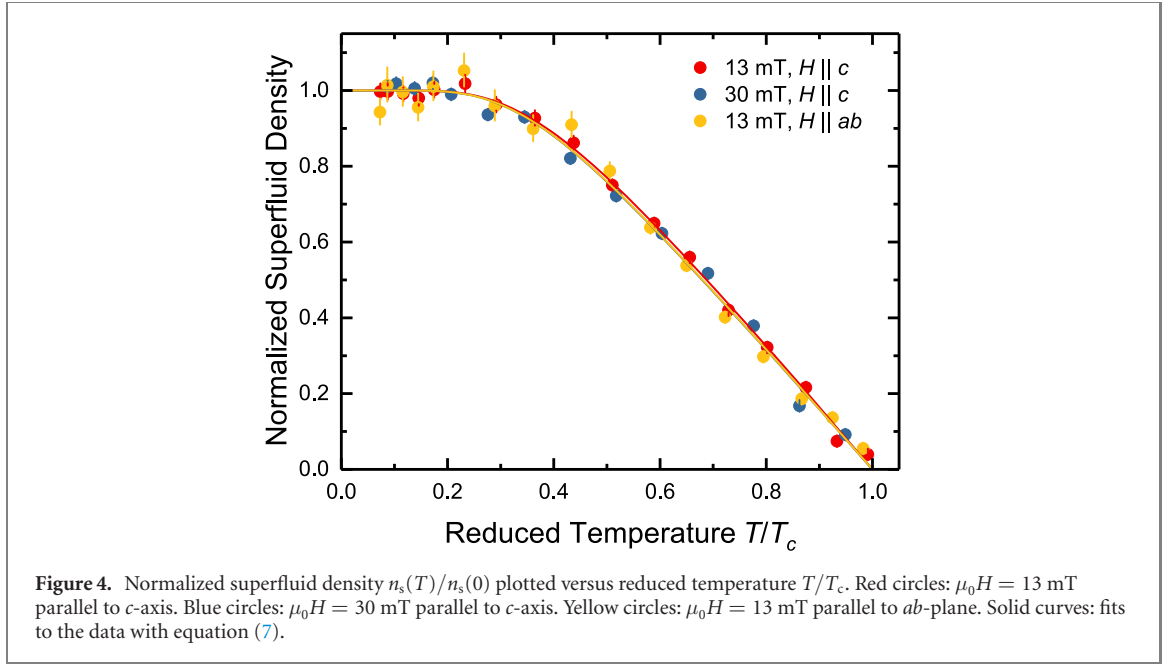
On the other hand, for a type-II superconductor, the internal field distribution can be described by penetration depth  $\lambda$ , which can be estimated based on  $\mu_0 H_{c1} = 9$  mT [28, 31]:

$$\mu_0 H_{c1} = \frac{\Phi_0}{4\pi\lambda^2} \left( \ln \frac{\lambda}{\xi} + 0.497 \right), \quad (4)$$

where  $\Phi_0 = 2.07 \times 10^{-15}$  Wb is the fluxoid quantum, and  $\xi$  is the coherence length. Based on the well-known relation

$$\mu_0 H_{c2} = \frac{\Phi_0}{2\pi\xi^2}, \quad (5)$$

we obtain  $\xi_c = 32.1$  nm and  $\xi_{ab} = 16.2$  nm, where  $\xi_c$  and  $\xi_{ab}$  are the coherence length parallel to  $c$ -axis and  $ab$ -plane, respectively [28]. Then we can estimate the value of  $\lambda$  along  $c$ -axis  $\lambda_c = 208.1$  nm and in  $ab$ -plane



$\lambda_{ab} = 242.0$  nm, and Ginzburg–Landau parameter  $\kappa = \lambda/\xi$  can be further derived, which shows  $\kappa_c = 6.5$  and  $\kappa_{ab} = 14.9$ . With  $\kappa > 5$ , and a not-too-small reduced magnetic field  $h = H/H_{c2} > 0.25/\kappa^{1.3}$ , one can calculate penetration depth  $\lambda$  more accurately using [31]

$$\sigma_{SC} = 0.172 \frac{\gamma \mu \Phi_0}{2\pi} (1-h) [1 + 1.21(1 - \sqrt{h})^3] \lambda^{-2}. \quad (6)$$

That is to say,  $\sigma_{SC}$  is proportional to  $\lambda^{-2}$ , and the complicated coefficient can be reduced by normalizing  $\sigma_{SC}(T)$  to  $\sigma_{SC}(0)$ .

Based on the London approximation, the superfluid density  $n_s(T)$  is also proportional to  $\lambda^{-2}$ . For a fully gapped  $s$ -wave superconductor,  $n_s$  can also be written as

$$\frac{\sigma_{SC}(T)}{\sigma_{SC}(0)} = \frac{n_s(T)}{n_s(0)} = 1 + 2 \int_{\Delta}^{\infty} \frac{\partial f}{\partial E} \frac{E}{\sqrt{E^2 - \Delta^2}} dE, \quad (7)$$

where  $n_0$  is the superfluid density at zero temperature,  $E$  is the energy difference above the Fermi energy,  $f = 1/[\exp(E/k_B T) + 1]$  is the Fermi function,  $k_B = 8.617 \times 10^{-5}$  eV K<sup>-1</sup> is the Boltzmann's constant, and  $\Delta$  is the gap function. For a fully-gapped  $s$ -wave superconductor, the temperature dependence of  $\Delta$  can be approximated by

$$\Delta(T) = \Delta_0 \tanh \left\{ 1.82 \left[ 1.018 \left( \frac{T_c}{T} - 1 \right) \right]^{0.51} \right\}, \quad (8)$$

where  $\Delta_0$  is the zero temperature gap [39].

The fitting results of normalized superfluid density  $n_s(T)/n_s(0)$  are plotted in figure 4. All three groups of data can be well fitted by single gap  $s$ -wave model. The derived zero temperature gap  $\Delta_0$  is 0.463(7) meV for  $\mu_0 H = 13$  mT along  $c$ -axis, 0.383(11) meV for  $\mu_0 H = 30$  mT along  $c$ -axis, and 0.458(15) meV for  $\mu_0 H = 13$  mT parallel to  $ab$ -plane. Interestingly, all three curves stack together and share the same behavior. Besides, unlike other anisotropic properties, even including the relaxation rates  $\sigma_{SC}$  for the superfluid density fitting, the two gap derived from two directions are very close (0.463(7) and 0.458(15) meV).

#### 4. Discussion

Previous work using  $\mu$ SR reported that two-gap model could describe the in-plane behavior of PbTaSe<sub>2</sub> better [23]. The evidence is not strong enough since there is no critical difference, and there is only one slightly increased point that influenced the conclusion. Our experiments can only be performed down to 0.25 K, just missing the critical point. Based on our results, PbTaSe<sub>2</sub> is a fully gapped superconductor, and whether it is single gap or two gap needs experiments to a lower temperature with dilution refrigerator.

Comparing our experimental results with previous theoretical calculations, we can find similar isotropic superconducting gap around  $H$  point in reciprocal space as defined in reference [25]. The magnitude of gap

derived from our results is also consistent with former reports [20, 23], but slightly smaller than the calculated values [25]. It could come from the suppression effect of external fields, which can be seen from the suppressed gap in our results. Although there are several other superconducting gaps derived by the theory, none of them is dominant in our experimental results. However, such a complicated band structure could account for the multi-band experimental results.

The anisotropy of relaxation rate in different directions suggest an anisotropic penetration depth  $\lambda$ . Since  $\lambda$  relates to effective mass, the strong anisotropy suggests a possible tensor effective mass. This point is further supported by the anisotropic  $\mu_0 H_{c2}$  and coherence length  $\xi$ . Noticed that spin-orbital coupling plays the most significant role at  $H$  point that induces topological properties [18, 20], such complex phenomenon is easy to expect.

Given that the dominant superconducting gap of  $\text{PbTaSe}_2$  is the isotropic gap around  $H$  point,  $\text{PbTaSe}_2$  is a 3D material. Besides, the fully gapped picture is also consistent with topological superconductivity. The presence of TRS is consistent with the picture of a 3D  $\mathbb{Z}_2$  topological superconductor [19, 21, 40]. Based on the classification of topological superconductivity [40, 41], besides TRS, particle–hole symmetry (PHS) and chiral symmetry (SLS) are also symmetries of great significance. It is important to study PHS and SLS of  $\text{PbTaSe}_2$  to understand its topological properties better. Furthermore, it would be more intriguing to study the role of the absence of inversion symmetry in its topological properties.

## 5. Conclusion

In summary, we performed ZF and TF- $\mu$ SR experiments on single crystalline  $\text{PbTaSe}_2$ . The preservation of TRS is confirmed by ZF- $\mu$ SR. The pairing symmetry is derived from TF- $\mu$ SR, indicating an isotropic 3D fully-gapped single-band picture, satisfying the requirement of topological superconductivity. The complicated band structure could account for the multi-band picture, but other bands are not dominant in superconductivity.

## Acknowledgments

This research was funded by the National Research and Development Program of China, No. 2017YFA0303104, the National Natural Science Foundations of China, No. 12174064 and 12174065, and the Shanghai Municipal Science and Technology (Major Project Grant Nos. 2019SHZDZX01 and 20ZR1405300).

## Data availability statement

All data that support the findings of this study are included within the article (and any supplementary files).

## ORCID iDs

P K Biswas  <https://orcid.org/0000-0002-7367-5960>

L Shu  <https://orcid.org/0000-0003-2725-1689>

## References

- [1] Bauer E and Sigrist M 2012 *Non-Centrosymmetric Superconductors (Lecture Notes in Physics)* vol 847 ed E Bauer and M Sigrist (Berlin: Springer)
- [2] Bauer E et al 2004 *Phys. Rev. Lett.* **92** 027003
- [3] Frigeri P A, Agterberg D F, Koga A and Sigrist M 2004 *Phys. Rev. Lett.* **92** 097001
- [4] Gor'kov L P and Rashba E I 2001 *Phys. Rev. Lett.* **87** 037004
- [5] Alicea J 2012 *Rep. Prog. Phys.* **75** 076501
- [6] Kim H et al 2018 *Sci. Adv.* **4** eaao4513
- [7] Scheurer M S and Schmalian J 2015 *Nat. Commun.* **6** 6005
- [8] Sun Z, Enayat M, Maldonado A, Lithgow C, Yelland E, Peets D C, Yaresko A, Schnyder A P and Wahl P 2015 *Nat. Commun.* **6** 6633
- [9] Qi X-L and Zhang S-C 2011 *Rev. Mod. Phys.* **83** 1057
- [10] Hillier A D, Quintanilla J and Cywinski R 2009 *Phys. Rev. Lett.* **102** 117007
- [11] Biswas P K et al 2013 *Phys. Rev. B* **87** 180503
- [12] Singh R P, Hillier A D, Mazidian B, Quintanilla J, Annett J F, Paul D M, Balakrishnan G and Lees M R 2014 *Phys. Rev. Lett.* **112** 107002



- [13] Barker J A T, Singh D, Thamizhavel A, Hillier A D, Lees M R, Balakrishnan G, Paul D M and Singh R P 2015 *Phys. Rev. Lett.* **115** 267001
- [14] Singh D, Barker J A T, Thamizhavel A, Paul D M, Hillier A D and Singh R P 2017 *Phys. Rev. B* **96** 180501
- [15] Singh D, Sajilesh K P, Paul D M, Hillier A D and Singh R P 2018 *Phys. Rev. B* **97** 100505
- [16] Hillier A D, Quintanilla J, Mazidian B, Annett J F and Cywinski R 2012 *Phys. Rev. Lett.* **109** 097001
- [17] Ali M N, Gibson Q D, Klimczuk T and Cava R J 2014 *Phys. Rev. B* **89** 020505
- [18] Bian G et al 2016 *Nat. Commun.* **7** 10556
- [19] Chang T-R et al 2016 *Phys. Rev. B* **93** 245130
- [20] Guan S-Y, Chen P-J, Chu M-W, Sankar R, Chou F, Jeng H-T, Chang C-S and Chuang T-M 2016 *Sci. Adv.* **2** e1600894
- [21] Chen P-J, Chang T-R and Jeng H-T 2016 *Phys. Rev. B* **94** 165148
- [22] Le T et al 2020 *Sci. Bull.* **65** 1349
- [23] Wilson M N, Hallas A M, Cai Y, Guo S, Gong Z, Sankar R, Chou F C, Uemura Y J and Luke G M 2017 *Phys. Rev. B* **95** 224506
- [24] Maeda S, Matano K and Zheng G-q 2018 *Phys. Rev. B* **97** 184510
- [25] Lian C-S, Si C and Duan W 2019 *Phys. Rev. B* **100** 235420
- [26] Pang G M et al 2016 *Phys. Rev. B* **93** 060506
- [27] Wang M X, Xu Y, He L P, Zhang J, Hong X C, Cai P L, Wang Z B, Dong J K and Li S Y 2016 *Phys. Rev. B* **93** 020503
- [28] Zhang C-L, Yuan Z, Bian G, Xu S-Y, Zhang X, Hasan M Z and Jia S 2016 *Phys. Rev. B* **93** 054520
- [29] Luke G M et al 1998 *Nature* **394** 558
- [30] Aoki Y et al 2003 *Phys. Rev. Lett.* **91** 067003
- [31] Brandt E H 2003 *Phys. Rev. B* **68** 054506
- [32] Suter A and Wojek B M 2012 *Phys. Procedia* **30** 69
- [33] Hayano R S, Uemura Y J, Imazato J, Nishida N, Yamazaki T and Kubo R 1979 *Phys. Rev. B* **20** 850
- [34] Kadono R, Imazato J, Matsuzaki T, Nishiyama K, Nagamine K, Yamazaki T, Richter D and Welter J-M 1989 *Phys. Rev. B* **39** 23
- [35] Clawson C W, Crowe K M, Rosenblum S S, Kohn S E, Huang C Y, Smith J L and Brewer J H 1983 *Phys. Rev. Lett.* **51** 114
- [36] Huddart B M, Onuorah I J, Isah M M, Bonfà P, Blundell S J, Clark S J, De Renzi R and Lancaster T 2021 *Phys. Rev. Lett.* **127** 237002
- [37] Camani M, Gygax F N, Rüegg W, Schenck A and Schilling H 1977 *Phys. Rev. Lett.* **39** 836
- [38] Shang T et al 2019 *Phys. Rev. B* **99** 184513
- [39] Carrington A and Manzano F 2003 *Physica C* **385** 205
- [40] Schnyder A P, Ryu S, Furusaki A and Ludwig A W W 2008 *Phys. Rev. B* **78** 195125
- [41] Kitaev A 2009 *AIP Conf. Proc.* **22** 22–30